Accepted Manuscript
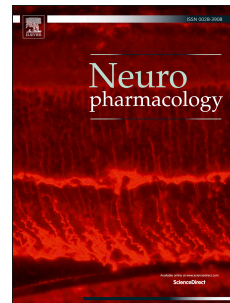
PcTx1 affords neuroprotection in a conscious model of stroke inhypertensive rats via selective inhibition of ASIC1a

Claudia A. McCarthy, Lachlan D. Rash, Irène R. Chassagnon, Glenn F. King, Robert E. Widdop

Please cite this article as: McCarthy, C.A., Rash, L.D., Chassagnon, I.R., King, G.F., Widdop, R.E., PcTx1 affords neuroprotection in a conscious model of stroke inhypertensive rats via selective inhibition of ASIC1a, *Neuropharmacology* (2015), doi: 10.1016/j.neuropharm.2015.08.040.

PcTx1 affords neuroprotection in a conscious model of stroke in hypertensive rats via selective inhibition of ASIC1a

Claudia A. McCarthy[1], Lachlan D. Rash[2], Irène R. Chassagnon[2], Glenn F. King[2]*, Robert E. Widdop[1]*

[1]Department of Pharmacology, Monash University, Clayton, Vic 3800, Australia
[2]Institute for Molecular Bioscience, The University of Queensland, St Lucia, QLD 4072, Australia

*Address for correspondence

Professor Glenn F. King, Institute for Molecular Bioscience, The University of Queensland, 306 Carmody Road, St Lucia, QLD 4072, Australia; Email: glenn.king@uq.edu.au.

Professor Robert E. Widdop Department of Pharmacology, Monash University, Clayton, Vic 3800, Australia; Email: robert.widdop@monash.edu.

Abstract

Acid-sensing ion channel 1a (ASIC1a) is the primary acid sensor in mammalian brain and plays a major role in neuronal injury following cerebral ischemia. Evidence that inhibition of ASIC1a might be neuroprotective following stroke was previously obtained using "PcTx1 venom" from the tarantula *Psalmopeous cambridgei*. We show here that the ASIC1a-selective blocker PcTx1 is present at only 0.4% abundance in this venom, leading to uncertainty as to whether the observed neuroprotective effects were due to PcTx1 blockade of ASIC1a or inhibition of other ion channels and receptors by the hundreds of peptides and small molecules present in the venom. We therefore examined whether pure PcTx1 is neuroprotective in a conscious model of stroke via direct inhibition of ASIC1a. A focal reperfusion model of stroke was induced in conscious spontaneously hypertensive rats (SHR) by administering endothelin-1 to the middle cerebral artery via a surgically implanted cannula. Two hours later, SHR were treated with a single intracerebroventricular (i.c.v.) dose of PcTx1 (1 ng/kg), an ASIC1a-inactive mutant of PcTx1 (1 ng/kg), or saline, and ledged beam and neurological tests were used to assess the severity of symptomatic changes. PcTx1 markedly reduced cortical and striatal infarct volumes measured 72 h post-stroke, which correlated with improvements in neurological score, motor function and preservation of neuronal architecture. In contrast, the inactive PcTx1 analog had no effect on stroke outcome. This is the first demonstration that selective pharmacological inhibition of ASIC1a is neuroprotective in conscious SHRs, thus validating inhibition of ASIC1a as a potential treatment for stroke.

1. Introduction

The severe oxygen depletion that occurs during ischemic stroke compels the brain to switch from oxidative phosphorylation to anaerobic glycolysis, which in turn leads to acidosis via increased lactate levels. The extracellular pH can fall from ~7.3 to 6.0–6.5 in the ischemic core under normoglycemic conditions, and it can drop to below 6.0 during severe ischemia (Isaev *et al.*, 2008; O'Bryant *et al.*, 2014; Xiong *et al.*, 2004). *In vivo* studies show that acidosis aggravates ischemic brain injury (Xiong *et al.*, 2004) and a direct correlation between brain acidosis and infarct size has been demonstrated (Xiong *et al.*, 2007). The pH reached during cerebral acidosis can activate acid-sensing ion channels (ASICs) and this activation has been suggested to play a critical role in stroke-induced neuronal injury (O'Bryant *et al.*, 2014; Xiong *et al.*, 2007).

ASICs were discovered in the late 1990s, almost 20 years after the observation that sensory neurons depolarise in response to a sudden drop in pH (Krishtal, 2003). Although they belong to the epithelial sodium channel/degenerin family of receptors, they are distinguished by their restriction to chordates, predominantly neuronal distribution, and activation by decreases in extracellular pH (Gründer *et al.*, 2010). Alternative splicing of four ASIC-encoding genes leads to the expression of six subunits (ASIC1a, ASIC1b, ASIC2a, ASIC2b, ASIC3, and ASIC4) that combine to form hetero- or homo-trimeric channels that differ in their pH sensitivity and tissue distribution (Wemmie *et al.*, 2006).

Postsynaptic ASIC1a channels are the dominant ASIC subtype in both human and rodent brain (Hoagland *et al.*, 2010; Li *et al.*, 2010). The pH for half-maximal activation ($pH_{0.5}$) of ASIC1a is 6.6 in human cortical neurons (Li *et al.*, 2010) and 6.4 in rat Purkinje neurons (Allen *et al.*, 2002) and consequently they are robustly activated by the decrease in extracellular pH that occurs during cerebral ischemia. Importantly, homomeric ASIC1a channels can mediate the uptake of Ca^{2+} in addition to Na^+ and protons (Gründer *et al.*, 2010). Thus, brain ASIC1a can contribute to the intracellular Ca^{2+} overload during stroke and may be at least partly responsible for the precipitous drop in intracellular pH from ~7 to as low as 6.15 during cerebral ischemia (Isaev *et al.*, 2008).

The most potent and selective blocker of ASIC1a described to date is PcTx1, a 40-residue

peptide isolated from the venom of the Trinidad Chevron tarantula, *Psalmopeous cambridgei* (Escoubas *et al.*, 2000). PcTx1 blocks rat ASIC1a (rASIC1a) with an IC_{50} of ~0.5 nM and ASIC1a/2b heteromers with an IC_{50} of ~3 nM, but it does not inhibit other ASIC homomers or heteromers. Several previous studies have claimed that PcTx1 is highly neuroprotective in rodent models of ischemic stroke (Pignataro *et al.*, 2007; Xiong *et al.*, 2004). For example, in a rat model of transient focal ischemia (middle cerebral artery occlusion; MCAO), i.c.v. injection of 'PcTx1 venom' 30 min before and after induction of ischemia reduced infarct size by 60% (Xiong *et al.*, 2004). Consistent with this being an effect mediated by ASIC1a, infarct size was similarly smaller by 61% in $ASIC1^{-/-}$ mice as compared to wild-type mice (Xiong *et al.*, 2004). These observations have improved our understanding of stroke pathophysiology and highlighted ASIC1a as a therapeutic candidate for the development of neuroprotective agents for treatment of stroke.

Surprisingly, the aforementioned studies did not use pure PcTx1 but rather the whole venom from the spider *P. cambridgei,* which contains PcTx1. Spider venoms are extremely complex chemical cocktails, containing hundreds to thousands of unique peptides (Escoubas *et al.*, 2006). The venom of *P. cambridgei* is no exception and it is known to contain modulators of TRPV1 and voltage-gated ion channels (Siemens, 2006) in addition to PcTx1. This raises the question as to whether the reported neuroprotective effect of 'PcTx1 venom' was due to block of ASIC1a by PcTx1 or unrelated pharmacological effects mediated by other venom components. Therefore, to address this question, we examined the neuroprotective efficacy of pure, recombinant PcTx1 in a conscious hypertensive rat model of transient MCAO. We show that a single dose of PcTx1 delivered 2 h after stroke dramatically reduces infarct size and restores normal levels of neurological and motor function. These effects are due specifically to inhibition of ASIC1a, as no neuroprotection was observed with a "disarmed" PcTx1 mutant peptide that can no longer inhibit the channel.

2. Materials and Methods

2.1 HPLC analysis of *P. cambridgei* venom

Reversed-phase (RP) HPLC analysis of crude *P. cambridgei* venom was performed using a Shimadzu Prominence system. One mg of venom was fractionated on a Zorbax SB300 reversed-

phase C18 column (4.6 × 250 mm, 5 μm, 300 Å) using a flow rate of 0.8 ml/min and the following gradient of solvent B (0.043% trifluoroacetic acid (TFA)in 90% acetonitrile) in solvent A (0.043% TFA in water): 10% solvent B for 2.5 min, 10–45% solvent B over 50 min, 45–70% solvent B over 5 min. The early eluting fraction was further analysed on a Thermo HyPurity C18 column (4.6 × 100 mm, 5 μm, 120 Å) using a gradient of 0% solvent B for 5 min then 0–15% solvent B over 15 min at a flow rate of 1 ml/min.

2.2 Peptide production

Recombinant PcTx1 and a double mutant analog were produced using an *E. coli* periplasmic expression system described previously (Klint, 2013). Briefly, synthetic genes encoding wild-type or mutant PcTx1, preceded by a TEV protease cleavage site, were produced by GeneArt (Regensburg, Germany) and subcloned into a variant of the pLicC-His$_6$-MBP periplasmic expression vector which enables periplasmic expression of target peptides as fusions to maltose binding protein (MBP). The His$_6$-MBP-PcTx1 fusion proteins were expressed in *E. coli* strain BL21(λDE3) and isolated from cell lysates by passage over Ni-NTA Superflow resin (QIAGEN). The His$_6$-MBP tag was then removed from the eluted fusion protein by cleavage with TEV protease. Recombinant PcTx1 (with an N-terminal serine added to facilitate TEV cleavage) was isolated to >95% purity using a final RP-HPLC step. We previously demonstrated that this recombinant peptide is equipotent with native PcTx1a (Saez *et al.*, 2011).

2.3 MALDI-TOF Mass Spectrometry

Peptide masses were confirmed by matrix assisted laser desorption ionisation–time of flight mass spectrometry (MALDI-TOF MS) using a Model 4700 Proteomics Bioanalyser (Applied Biosystems, CA, USA). Peptide samples were mixed (1:1, v:v) with α-cyano-4-hydroxy-cinnamic acid matrix (5 mg/ml in 50/50 acetonitrile/H$_2$O) and MALDI-TOF spectra were collected in positive reflector mode. All masses given are for the monoisotopic M+H$^+$ ions.

2.4 Electrophysiology

Two-electrode voltage clamp (TEVC) was carried out using *Xenopus* oocytes as previously described (Schroeder *et al.*, 2014). cRNA encoding rat ASIC1a (rASIC1a) was synthesized using an mMessage mMachine cRNA transcription kit and healthy stage V-VI oocytes injected with 4

ng rASIC1a cRNA (40 nL of 100 ng/uL). All experiments were performed at room temperature (18–21°C) in ND96 solution containing 0.1% fatty acid free-bovine serum albumin (BSA). Changes in extracellular pH were induced using a microperfusion system that allowed local, rapid exchange of solutions. HEPES was replaced by MES to buffer the pH 6 stimulus solution. Peptides were dissolved in ND96 solution (pH7.45) containing 0.1% BSA to prevent adsorption onto tubing.

2.5 Cannulae implantation

Male spontaneously hypertensive rats (SHR) (~ 20 weeks of age; 300–350g) were anaesthetised with ketamine (75 mg/kg; Sigma)/xylazine (10 mg/kg; Troy; i.p). A 23-gauge stainless steel guide cannula was stereotaxically implanted to sit 3 mm dorsal to the right middle cerebral artery in the piriform cortex. An additional cannula was implanted into the left lateral ventricle (–0.8 mm anterior, +1.5 mm lateral, and –3.2 mm ventral relative to Bregma) which was left exposed to allow a bolus dose of drug to be administered 2 h after stroke. The animals were housed individually and were allowed a 5-day recovery period prior to the induction of stroke. All animal care and procedures were approved by the Monash University Animal Ethics Committee. The minimum number of animals were used and, where possible, an *in vitro* approach was applied.

2.6 Drug treatments

SHR (~20 weeks of age; 300–350 g) were randomly allocated to one of several treatment groups so the experimenter was blind to all treatments. Out of the thirty animals stroked in this study, one animal was excluded because it did not reach the appropriate level of stroke. In addition, three animals were excluded because they had a stroke that was greater than a grade-4 stroke. All excluded animals were humanely sacrificed immediately after the final injection of endothein-1 (ET-1). The remaining animals received either PcTx1 (1 ng/kg; $n = 9$), inactive mutant PcTx1 (1 ng/kg; $n = 7$), or vehicle (saline) ($n = 10$). All drugs were administered by intracerebroventricular (i.c.v.) injection 2 h after stroke via a previously implanted guide cannula using a 30-gauge injector protruding 3 mm into the lateral ventricle. Drugs were dissolved in saline and infused in a volume of 3 μl over 3 min.

4

2.7 Stroke induction

During stroke induction, animals were placed in a clear Perspex box to allow observation. Stroke was induced in conscious animals by inserting a 30-gauge injector protruding 3 mm below the end of the previously implanted guide cannula and ET-1 (20 pmol/µl in saline; AusPep) was injected at a rate of 0.2 µl every 30 s until the animal exhibited behavioural changes associated with the desired level of stroke, as described previously (McCarthy *et al.*, 2009; McCarthy *et al.*, 2012; McCarthy *et al.*, 2014).)Typical behaviors that were observed were continuous contralateral and ipsilateral circling; clenching, dragging, or failure to extend the forelimb contralateral to the side of ET-1 infusion; chewing and jaw flexing and shuffling with forepaws. Each stroke was graded based on these pre-determined behavioral changes using a scale of 1 to 4, with 1 being a mild stroke and 4 being a severe stroke. Only rats with a grade-4 level of stroke, exhibiting at least five of the aforementioned behaviors, were used for the purpose of this investigation.

2.8 Assessment of functional outcome

2.8.1 Ledged beam test

Stroke-induced changes in motor coordination were examined by assessing the animal's dependence on the underhanging wider ledge of a gradually narrowing beam as previously described (McCarthy *et al.*, 2012; McCarthy *et al.,* 2009; McCarthy *et al.*, 2014). Naïve rats are able to traverse the central portion of the beam without using the underhanging ledges for support. Stroked rats rely on the lower ledge for support on the impaired side and take more steps on the ledge. Animals were trained to traverse the beam on the day prior to surgical implantation of the cannula. The ledged beam test was conducted immediately before stroke induction, at 24 h (day 1) and ~70 h after stroke induction (day 3). The number of steps taken on the lower ledge (errors) by each foot was recorded and expressed as a percentage of the total number of footsteps taken and recorded as percentage error. All values were compared to pre-stroke performance, and therefore each rat acted as its own control.

2.8.2 Neurological test

Postural abnormalities were assessed by grading the severity of thorax twisting and the angle of forelimb extension when the rat is elevated by the tail above a flat surface (Yamamoto *et al.*,

5

1988). Thorax twisting was scored on a scale of 0 to 3, with 0 representing no twisting behavior and 3 representing severe twisting. Forelimb extension was also scored on a scale of 0 to 3, with 0 representing full contralateral forelimb extension, and 3 representing a complete failure to extend the contralateral forelimb. Both scores were summed to give a total neurological deficit score, where the maximum total score an animal could achieve was 6. A total score of zero indicated that the animal was normal with no neurological deficit evident, whereas a total score of 6 indicated sever neurological deficit. The test was conducted prior to surgery, immediately before stroke, and 24 h and 72 h after stroke induction.

2.9 Histology

2.9.1 Quantification of ischemic damage

At 72 h after stroke rats were re-anaesthetised with ketamine (75 mg/kg; Sigma)/xylazine (10 mg/kg; Troy) and transcardially perfused with physiologically buffered saline (0.1 M PBS; pH 7.4) at a rate of 25 ml/min. Brains were then removed, snap frozen, and sectioned for image analysis to determine infarct size, as previously described (Callaway *et al*., 2000; McCarthy *et al*., 2009; McCarthy *et al*., 2012; McCarthy *et al*., 2014).

2.9.2 Immunohistochemical staining

Neuronal integrity was assessed using a neuron-specific marker, NeuN antibody (1:500 dilution, Chemicon), which is a DNA-binding protein that binds to the nucleus of neurons. In addition, cells undergoing apoptosis were identified using an antibody against a common mediator in the apoptotic pathway, cleaved Caspase-3 (1:200 dilution, AbCAM). Frozen coronal cryostat sections (16 µm) were post-fixed using 100% acetone for 10 min. Slides were incubated overnight with either the NeuN or cleaved Caspase-3 antibody at 4˚C. Sections were then incubated at room temperature for 2 h with a fluorescently labelled secondary antibody: Alexa 488 was used for NeuN (1:500 dilution, Invitrogen) and Alexa 568 for cleaved Caspase-3 (1:500 dilution, Invitrogen). The number of immunopositive cells were counted within six 1-mm^2 sites that were randomly imaged on the ipsilateral and contralateral hemispheres. Data are expressed as the average number of immunopositive cells per mm^2.

2.10 Statistical Analysis

Results are presented as mean ± standard deviation of the mean (SD). The ledged beam test, neurological score, and systolic blood pressure were analysed using a two-way repeated measures analysis of variance (ANOVA). Neuronal expression (NeuN-positve cells) and apoptosis (caspase-3-positive cells) were analysed by two way ANOVA, while infarct area was analysed using a one-way ANOVA. Post hoc testing, corrected for multiple comparisons, was performed using Tukey's test. A P value < 0.05 was considered to be statistically significant. Data analysis was performed using GraphPad Prism (Version 6).

3. Results

3.1 Complexity of *P. cambridgei* venom ("PcTx1 venom")

Venom from *P. cambridgei* has previously been used as a substitute for PcTx1 in stroke studies (Li *et al.*, 2010; Pignataro *et al.*, 2007; Xiong *et al.*, 2004) due to the lack of a commercial supplier. Since spider venoms are extremely complex mixtures of salts, small molecules, peptides and proteins (King *et al.*, 2013), we decided to examine the relative abundance of PcTx1 peptide in *P. cambridgei* venom. Fractionation of *P. cambridgei* venom using RP-HPLC yielded a complicated chromatogram with more than 50 peaks, indicative of a highly complex venom (black trace in Fig 1A). The peak corresponding to native PcTx1 was confirmed by comparison with the retention time of pure, recombinant PcTx1 eluted under the same conditions (grey trace in Fig. 1A) as well as MALDI-TOF mass spectrometry (observed $M+H^+ = 4687.32$, calculated $M+H^+ = 4687.21$). Integration of each of the peaks in the venom chromatogram revealed that PcTx1 constitutes only ~0.4% of the total venom based on absorbance at 214 nm. We conclude that PcTx1 is found at very low abundance in *P. cambridgei* venom, and therefore one cannot definitively conclude that the pharmacological effects evoked by "PcTx1 venom" in stroke studies are due solely to PcTx1 inhibition of ASIC1a.

3.2 Activity of recombinant PcTx1 and "disarmed" mutant

In order to examine the neuroprotective effects of pure PcTx1, we produced recombinant PcTx1 as described previously (Saez *et al.*, 2011) as well as a double mutant version of the peptide that was designed to be inactive on ASIC1a. Our previous structure-function studies of PcTx1 (Saez *et al.*, 2011) as well as crystal structures of the complex formed between PcTx1 and chicken

ASIC1 (Baconguis, 2012; Dawson *et al.*, 2012) indicate that residues Arg27 and Val32 are important for PcTx1 inhibition of ASIC1a. Thus, we produced an R27A/V32A double mutant peptide (Fig. 1B) and examined the ability of this analogue to inhibit rASIC1a. Electrophysiological analysis indicated that recombinant wild-type PcTx1 inhibits rASIC1 with an IC_{50} of 0.82 ± 0.19 nM, consistent with literature values (Escoubas *et al.*, 2000; Saez *et al.*, 2011), whereas the R27A/V32A mutant is essentially inactive with an $IC_{50} > 10\,\mu M$ (i.e., >10,000-fold lower potency) (Fig. 1C). Thus, the disarmed R27A/V32A mutant PcTx1 provides a valuable control to determine whether the *in vivo* effects of PcTx1 are due to inhibition of ASIC1a.

3.3 Effect of PcTx1 on infarct size following MCAO

A single dose (1 ng/kg) of PcTx1 delivered i.c.v. 2 h after MCAO had a dramatic impact on infarct size (Fig. 2). The cortical infarct volume measured 72 h after MCAO was ~70% smaller in PcTx1-treated animals (32 ± 30 mm^3) compared to control animals (108 ± 71 mm^3; P<0.05). Striatal infarct volume appeared lower in PcTx1-treated animals (24.0 ± 8.4 mm^3) compared to control animals (39 ± 27 mm^3), but this did not reach statistical significance. In contrast with native PcTx1, the disarmed PcTx1 mutant had no effect on the severity of cortical or striatal damage. The individual infarct volume areas for each group are also shown in (Fig 2). We conclude that PcTx1 treatment reduces infarct size after stroke due to pharmacological blockade of ASIC1a.

3.4 Effect of PcTx1 on motor deficits following MCAO

Compared to pre-stroke measurements, there was a pronounced motor deficit in vehicle-treated SHRs at both 1 and 3 days after stroke (i.e., >40% error in the ledged-beam test; Fig. 3A). PcTx1 treatment (1 ng/kg i.c.v.) significantly reduced the severity of motor deficit at 1 and 3 days after stroke compared to control rats (<10 % error in ledged-beam test; P<0.01 versus corresponding time points in vehicle-treated group) (Fig. 3A). In accordance with the histological data, the inactive PcTx1 mutant had no effect on motor deficits after stroke (Fig. 3A).

8

3.5 Effect of PcTx1 on neurological scores following MCAO

A significant neurological deficit was observed at 1 and 3 days after ET-1 induced stroke in both the control animals (1 day: 4.0 ± 1.9 ; 3 days: 3.3 ± 2.0 ; $P<0.01$ versus pre-stroke deficit) and animals receiving inactive PcTx1 mutant (1 day: 4.9 ± 1.5; 3 days: 3.9 ± 1.3; $P<0.01$ versus pre-stroke deficit). Remarkably, there was very little sign of neurological deficit at either time point after stroke (1 day: 0.7 ± 1.0; 3 days: 0.7 ± 0.9; $P<0.01$ versus corresponding time points in vehicle-treated group; Fig. 3B) in animals that received PcTx1.

3.6 Effect of PcTx1 on neuronal survival following MCAO

The number of neurons detected by NeuN-immunopositive staining was lower in the infarcted (ipsilateral) hemisphere compared to the non-infarcted (contralateral) hemisphere in both vehicle-treated animals and those receiving the inactive PcTx1 mutant (Fig. 4), although only the latter reached statistical significance ($P<0.01$). Loss of NeuN-positive staining was much less evident in in the occluded hemisphere of animals treated with PcTx1 ($P<0.05$), suggestive of improved neuronal survival in these animals.

The number of cells undergoing apoptosis in the occluded hemisphere of stroked SHRs receiving either vehicle or inactive PcTx1 was higher than in the contralateral hemisphere (Fig. 5), in accordance with the decreased neuronal survival in the same hemisphere (Fig. 4). Treatment with PcTx1 had an anti-apoptotic effect in the occluded hemisphere as evidenced by a blunting of the stroke-induced increase in the number of cells positive for cleaved caspase-3 (Fig. 5).

4. Discussion

In the present study, we demonstrated that PcTx1 affords both functional and anatomical neuroprotection following induction of stroke in conscious SHR. These protective effects were absent in animals treated with a PcTx1 mutant that lacks activity against ASIC1a, thus demonstrating, for the first time, that the neuroprotection afforded by PcTx1 peptide is due to selective inhibition of ASIC1a.

Stroke is the is the second leading cause of death worldwide (Moskowitz *et al.*, 2010; Woodruff *et al.*, 2011) and the leading cause of disability in industrialized countries (Liu *et al.*, 2012). The use of recombinant tissue plasminogen activator (rtPA) to help restore blood flow to the ischemic region is the only approved agent for treatment of acute stroke and it is used in only 3–4% of all stroke patients (Besancon *et al.*, 2008) due to its narrow therapeutic window and the risk of inducing intracranial hemorrhage (Moskowitz *et al.*, 2010). Thus, there is intense interest in developing new approaches for treatment of stroke victims.

Ischemia-induced acidosis causes neuronal injury independently of the activation of voltage-gated calcium channels and glutamate receptors. Activation of ASICs appears to represent a key mechanism by which a reduction in the pH of ischemic tissue leads to calcium influx and excitotoxicity (O'Bryant *et al.*, 2014). This distinct mechanism of excitotoxicity might in part explain the failure of NMDA receptor antagonists in clinical trials against stroke (O'Bryant *et al.*, 2014). Infarct size is reduced by ~60% in ASIC1a knockout mice (Xiong *et al.*, 2004) which suggests that ASIC1a, the primary ASIC subtype in rodent and human brain (Li *et al.*, 2010), is a key contributor to the pathological events induced by ischemic stroke.

Several studies have attempted to demonstrate a causal role for ASIC1a in the neurodegeneration induced by cerebral ischemia by employing nonselective small-molecule ASIC1 inhibitors such as flurbiprofen (Mishra *et al.*, 2010; Mishra *et al.*, 2011) and aspirin (Wang *et al.*, 2012), "PcTx1 venom" (Pignataro *et al.*, 2007; Xiong *et al.*, 2004), or genetic ablation of ASIC1a (Xiong *et al.*, 2004) as a means of reducing ASIC1a function. NSAIDs such as flurbiprofen and aspirin are weak, nonselective inhibitors of ASIC1a and they affect a myriad of other biological targets. Genetic ablation of an ion channel can give rise to compensatory regulation of related subtypes of the target channel with unknown consequences. As shown here, "PcTx1 venom" contains only a very small amount of PcTx1 amongst many other venom peptides that likely affect a wide array of voltage- and ligand-gated ion channels (King *et al.*, 2013). Thus, none of these approaches provides definitive evidence that acute pharmacological inhibition of ASIC1a is likely to be neuroprotective in ischemic stroke.

Tarantula venoms are exceptionally complex chemical cocktails dominated by disulfide-rich neurotoxic peptides (Herzig *et al.*, 2013; King *et al.*, 2013). The primary molecular targets of these peptides are neuronal voltage-gated calcium, sodium and potassium channels (Herzig *et al.*, 2013). We showed here that PcTx1 constitutes a very minor proportion (~0.4%) of *P. cambridgei* venom, which equates to a concentration of 40–80 μM in crude venom. In comparison, the venom of this spider is known to contain modulators of TRPV1 and voltage-gated potassium channels at concentrations in the 0.2–1.7 mM range (Choi, 2004; Siemens, 2006). Thus, the *in vivo* effects of "PcTx1 venom" are likely to be due to the combined effects from a wide variety of venom peptides, rather than solely due to PcTx1inhibition of ASIC1a. Thus, we strongly recommend against using "PcTx1 venom" as a method to selectively inhibit ASIC1a *in vivo*.

We examined the effect of pure, recombinant PcTx1 using a model of cerebral ischemia that closely mimics the clinical setting in that animals are conscious while stroke is induced. This avoids the confounding effects of anaesthesia, which are known to be neuroprotective (McCarthy *et al.*, 2012; McCarthy *et al.*, 2009; McCarthy *et al.*, 2014). Furthermore, MCAO was performed on hypertensive animals, since high blood pressure is an important risk factor for stroke. Additionally, the hemodynamic changes induced via targeted application of ET-1 are representative of human stroke, with blood flow reduction at the onset of ET-1 administration resulting in complete occlusion of the vessel, which begins to resolve over a period of 30–40 min after stroke with blood flow returning to normal over the following 16–22 h (Mecca *et al.*, 2009). The region of damage resulting from this transient model of stroke is characterised by a necrotic core of severely impacted tissue, surrounded by an ischemic penumbra of compromised but salvageable neurons, which over time will gradually undergo apoptotic cell death in the absence of therapeutic intervention. When administered centrally 2 h after stroke, a single nanogram dose of pure PcTx1 almost halved the volume of neuronal damage in SHRs, as measured three days post-insult. PcTx1 not only afforded protection in the cortical region (ischemic penumbra), but tended to reduce the severity of damage in the striatal core (i.e., tissue directly impacted by hypoxia), which is generally considered resistant to therapeutic intervention.

In previous studies, "PcTx1 venom" was administered at a dose of 10 ng/kg in mice at 5 h after transient MCAO (Pignataro *et al.*, 2007), and immediately before and after stroke induction in rats with transient MCAO, with the rat brain concentration estimated at ~50 ng/ml (Xiong *et al.*, 2004). Given that PcTx1 represents ~0.4% of crude *P. cambridgei* venom, the estimated brain concentration of PcTx1 in these studies (0.2 ng/ml, ~0.03 nM) would have been ~15–30-fold lower than the reported IC_{50} for PcTx1 inhibition of rASIC1a (Escoubas *et al.*, 2000; Saez *et al.*, 2011). This dose would lead to only minimal inhibition of brain ASIC1a (<5%). Thus, it is unclear whether the small amount of PcTx1 administered in previous studies (Pignataro *et al.*, 2008; Xiong *et al.*, 2004) was solely responsible for the observed neuroprotective effects or whether they are due to the combined effect of several venom components. In contrast, the dose of PcTx1 used in the current study equates to a brain concentration of ~1.2 nM, which should inhibit brain ASIC1a activity by >60%.

Earlier findings (Pignataro *et al.*, 2008; Xiong *et al.*, 2004) showed that, "PcTx1 venom" markedly reduced infarct volume when assessed 24 h after stroke, although no functional correlates were examined. Notably, in the current study, the preservation of brain tissue by PcTx1 was reflected symptomatically, with PcTx1-treated animals experiencing less motor impairment and reduced neurological deficit following stroke. Moreover, the absence of neuroprotection in animals receiving inactive PcTx1 mutant provides strong evidence that the neuroprotection afforded by PcTx1 is due specifically to its ability to inhibit ASIC1a. PcTx1 (IC_{50} ~0.5-1 nM) is a considerably more potent inhibitor of ASIC1a than small molecules such as amiloride (IC_{50} ~10 µM) (Gründer *et al.*, 2010), flurbiprofen (IC_{50} ~350 µM) (Voilley *et al.*, 2001), and sinomenine (IC_{50} ~0.27 M) (Wu *et al.*, 2011), and it is also much more selective. Thus, the neuroanatomical and behavioural protection afforded by PcTx1 in the current study more convincingly demonstrates the therapeutic potential of ASIC1a blockade as a treatment for stroke.

Our immunohistochemical analysis indicated that stroke markedly increased the number of cells undergoing apoptosis in the ipsilateral hemisphere, but the number of caspase-3 positive cells was reduced in PcTx1-treated animals. In the future, it would be of interest to use other apoptotic assays, such as terminal deoxynucleotidyl transferase dUTP nick-end labeling (TUNEL), to

examine the PcTx1 treatment effect, particularly given that some studies have shown that non-apoptotic cells such as reactive astrocytes, macrophages/microglia and neutrophils express caspase-3 at 72 h after stroke (Nag *et al.*, 2005; Wagner *et al.*, 2011). In any case, the increase in caspase-3 immunostaining in the area directly affected by ischemia is consistent with the stroke-induced loss of neuronal integrity, as identified by NeuN in the vehicle-treated animals, which we have consistently reported (McCarthy *et al.*, 2009; McCarthy *et al.*, 2012; McCarthy *et al.*, 2014). Furthermore, treatment with PcTx1 blunted the loss of NeuN staining, signifying a preservation of neuronal survival. Thus, PcTx1 prevented apoptosis following MCAO, which is in keeping with the conservation of neuronal architecture and is reflected by both the histological and behavioural data.

The current study provides striking proof-of-principle that inhibition of central ASIC1a interrupts the pathological events occurring after MCAO. However, the elucidation of the time course of neuroprotection using clinically relevant routes of drug administration in several animal models is required before clinical translation of these findings into humans (Fisher *et al.*, 2009).

Conclusion

Selective inhibition of brain ASIC1a with pure PcTx1 peptide provides functional- and anatomical- neuroprotection following induction of stroke in conscious SHR. These findings indicate that ASIC1a is an exciting therapeutic target after an ischemic event.

Conflict(s) of interest

None

References

Allen NJ, Attwell D (2002). Modulation of ASIC channels in rat cerebellar Purkinje neurons by ischaemia-related signals. *J. Physiol.* **543**(2)**:** 521–529.

Baconguis IEG, E. (2012). Structural plasticity and dynamic selectivity of acid-sensing ion channel–spider toxin complexes. *Nature* **489:** 400–405.

Besancon E, Guo S, Lok J, Tymianski M, Lo EH (2008). Beyond NMDA and AMPA glutamate receptors: emerging mechanisms for ionic imbalance and cell death in stroke. *Trends Pharmacol. Sci.* **29**(5)**:** 268–275.

Choi S, Parentb, R., Guillaume, C., Deregnaucourt, C., Delarbre, C., Ojcius, D., Montagne, J.J., Celerier, M., , Phelipot, A., Amiche, M., Molgog, J., Camadro, J.M., Guette, C. (2004). Isolation and characterization of psalmopeotoxin I and II: two novel antimalarial peptides from the venom of the tarantula *Psalmopoeus cambridgei. FEBS Lett.* **572**(1–3)**:** 109–117.

Dawson R, Benz J, Stohler P, Tetaz T, Joseph C, Huber J*, et al.* (2012). Structure of the acid-sensing ion channel 1 in complex with the gating modifier psalmotoxin 1. *Nat. Commun.* **3:** 936.

Escoubas P, De Weille JR, Lecoq A, Diochot S, Waldmann R, Champigny G*, et al.* (2000). Isolation of a tarantula toxin specific for a class of proton-gated Na^+ channels. *J. Biol. Chem.* **275**(33)**:** 25116–25121.

Escoubas P, Sollod B, King GF (2006). Venom landscapes: mining the complexity of spider venoms via a combined cDNA and mass spectrometric approach. *Toxicon* **47**(6)**:** 650–663.

Fisher M, Feuerstein G, Howells DW, Hurn PD, Kent TA, Savitz SI*, et al.* (2009). Update of the stroke therapy academic industry roundtable preclinical recommendations. *Stroke* **40**(6)**:** 2244–2250.

Gründer S, Chen X (2010). Structure, function, and pharmacology of acid-sensing ion channels (ASICs): focus on ASIC1a. *Int. J. Physiol. Pathophysiol. Pharmacol.* **2**(2)**:** 73–94.

Herzig V, King GF (2013). The neurotoxic mode of action of venoms from the spider family Theraphosidae. In: Nentwig W (ed). *Spider Ecophysiology*, Heidelberg: Springer-Verlag. pp 203–215.

Hoagland EN, Sherwood TW, Lee KG, Walker CJ, Askwith CC (2010). Identification of a calcium permeable human acid-sensing ion channel 1 transcript variant. *J. Biol. Chem.* **285**(53)**:** 41852–41862.

Isaev NK, Stelmashook EV, Plotnikov EY, Khryapenkova TG, Lozier ER, Doludin YV*, et al.* (2008). Role of acidosis, NMDA receptors, and acid-sensitive ion channel 1a (ASIC1a) in neuronal death induced by ischemia. *Biochemistry (Mosc)* **73**(11)**:** 1171–1175.

King GF, Hardy MC (2013). Spider-venom peptides: structure, pharmacology, and potential for control of insect pests. *Annu. Rev. Entomol.* **58:** 475–496.

Klint JK, Senff S, Saez NJ, Seshadri R, Lau HY, Bende NS, Undheim EAB, Rash LD, Mobli M, King GF (2013). Production of recombinant disulfide-rich venom peptides for structural and functional analysis via expression in the periplasm of *E. coli PLoS One* **8** e63865.

Krishtal O (2003). The ASICs: signaling molecules? Modulators? *Trends Neurosci.* **26**(9)**:** 477–483.

Li M, Inoue K, Branigan D, Kratzer E, Hansen JC, Chen JW, *et al.* (2010). Acid-sensing ion channels in acidosis-induced injury of human brain neurons. *J. Cereb. Blood Flow Metab.* **30**(6)**:** 1247–1260.

Liu R, Yuan H, Yuan F, Yang SH (2012). Neuroprotection targeting ischemic penumbra and beyond for the treatment of ischemic stroke. *Neurol. Res.* **34**(4)**:** 331–337.

McCarthy CA, Vinh A, Broughton BR, Sobey CG, Callaway JK, Widdop RE (2012). Angiotensin II type 2 receptor stimulation initiated after stroke causes neuroprotection in conscious rats. *Hypertension* **60**(6)**:** 1531–1537.

McCarthy CA, Vinh A, Callaway JK, Widdop RE (2009). Angiotensin AT_2 receptor stimulation causes neuroprotection in a conscious rat model of stroke. *Stroke* **40**(4)**:** 1482–1489.

McCarthy CA, Vinh A, Miller AA, Hallberg A, Alterman M, Callaway JK, Widdop RE. (2014). Direct angiotensin AT2 receptor stimulation using a novel AT2 receptor agonist, compound 21, evokes neuroprotection in conscious hypertensive rats. *PLoS One* **9**(4)**:** e95762.

Mecca AP, O'Connor TE, Katovich MJ, Sumners C (2009). Candesartan pretreatment is cerebroprotective in a rat model of endothelin-1-induced middle cerebral artery occlusion. *Exp. Physiol.* **94**(8)**:** 937–946.

Mishra V, Verma R, Raghubir R (2010). Neuroprotective effect of flurbiprofen in focal cerebral ischemia: the possible role of ASIC1a. *Neuropharmocology* **59**(7–8)**:** 582–588.

Mishra V, Verma R, Singh N, Raghubir R (2011). The neuroprotective effects of NMDAR antagonist, ifenprodil and ASIC1a inhibitor, flurbiprofen on post-ischemic cerebral injury. *Brain Res.* **1389:** 152–160.

Moskowitz MA, Lo EH, Iadecola C (2010). The science of stroke: mechanisms in search of treatments. *Neuron* **67**(2)**:** 181–198.

Nag S, Papneja T, Venugopalan R, Stewart DJ (2005). Increased angiopoietin2 expression is associated with endothelial apoptosis and blood-brain barrier breakdown. *Lab. Invest.* **85**(10)**:** 1189-1198.

O'Bryant Z, Vann KT, Xiong ZG (2014). Translational strategies for neuroprotection in ischemic stroke—focusing on acid-sensing ion channel 1a. *Transl. Stroke Res.* **5**(1)**:** 59–68.

Pignataro G, Meller R, Inoue K, Ordonez AN, Ashley MD, Xiong Z*, et al.* (2008). *In vivo* and *in vitro* characterization of a novel neuroprotective strategy for stroke: ischemic postconditioning. *J. Cereb. Blood Flow Metab.* **28**(2)**:** 232–241.

Pignataro G, Simon RP, Xiong ZG (2007). Prolonged activation of ASIC1a and the time window for neuroprotection in cerebral ischaemia. *Brain* **130**(1)**:** 151–158.

Saez NJ, Mobli M, Bieri M, Chassagnon IR, Malde AK, Gamsjaeger R*, et al.* (2011). A dynamic pharmacophore drives the interaction between psalmotoxin-1 and the putative drug target acid-sensing ion channel 1a. *Mol. Pharmacol.* **80:** 796–808.

Schroeder CI, Rash LD, Vila-Farres X, Rosengren KJ, Mobli M, King GF*, et al.* (2014). Chemical synthesis, 3D structure, and ASIC binding site of the toxin mambalgin-2. *Angewandte Chemie* **53**(4)**:** 1017–1020.

Siemens J, Zhou, S., Piskorowski, R., Nikai, T., Lumpkin3, E., Basbaum, A., King, D., Julius, D. (2006). Spider toxins activate the capsaicin receptor to produce inflammatory pain. *Nature* **444**(9)**:** 208–212.

Voilley N, de Weille J, Mamet J, Lazdunski M (2001). Nonsteroid anti-inflammatory drugs inhibit both the activity and the inflammation-induced expression of acid-sensing ion channels in nociceptors. *J. Neurosci.* **21**(20)**:** 8026–8033.

Wagner DC, Riegelsberger UM, Michalk S, Hartig W, Kranz A, Boltze J (2011). Cleaved caspase-3 expression after experimental stroke exhibits different phenotypes and is predominantly non-apoptotic. *Brain Res.* **1381:** 237–242.

Wang W, Ye SD, Zhou KQ, Wu LM, Huang YN (2012). High doses of salicylate and aspirin are inhibitory on acid-sensing ion channels and protective against acidosis-induced neuronal injury in the rat cortical neuron. *J. Neurosci. Res.* **90**(1)**:** 267–277.

Wemmie JA, Price MP, Welsh MJ (2006). Acid-sensing ion channels: advances, questions and therapeutic opportunities. *Trends Neurosci.* **29**(10)**:** 578–586.

Woodruff TM, Thundyil J, Tang SC, Sobey CG, Taylor SM, Arumugam TV (2011). Pathophysiology, treatment, and animal and cellular models of human ischemic stroke. *Mol. Neurodegener.* **6**(1)**:** 11.

Wu WN, Wu PF, Chen XL, Zhang Z, Gu J, Yang YJ*, et al.* (2011). Sinomenine protects against ischaemic brain injury: involvement of co-inhibition of acid-sensing ion channel 1a and L-type calcium channels. *Br. J. Pharmacol.* **164**(5)**:** 1445–1459.

Xiong ZG, Chu XP, Simon RP (2007). Acid sensing ion channels—novel therapeutic targets for ischemic brain injury. *Front. Biosci.* **12:** 1376–1386.

Xiong ZG, Zhu XM, Chu XP, Minami M, Hey J, Wei WL*, et al.* (2004). Neuroprotection in ischemia: blocking calcium-permeable acid-sensing ion channels. *Cell* **118**(6)**:** 687–698.

Figure Legends

Figure 1: (A) RP-HPLC chromatograms of *P. cambridgei* venom (black trace) and recombinant PcTx1 (grey trace) highlighting the chemical complexity of the venom and the minor abundance of PcTx1. The large inset shows re-fractionation of the early-eluting components on a different column in order to reveal the hidden complexity in this region of the chromatogram. The small inset is a MALDI-TOF MS spectrum of native PcTx1 (observed $M+H^+$ = 4687.32, calculated $M+H^+$ = 4687.21). (B) RP-HPLC chromatogram showing the purity of the recombinant R27A/V32A double mutant PcTx1. (C) Concentration-effect curves for inhibition of rASIC1a expressed in *Xenopus* oocytes by recombinant PcTx1 and the R27A/V32A double mutant peptide. Calculated IC_{50} values are listed on the figure.

Figure 2. Infarct volume after MCAO. Histological sections showing typical infarcted region (darker area) and non-infarcted region from SHR that were treated with (A) vehicle, (B) PcTx1 (1 ng/kg i.c.v.), or (C) inactive PcTx1 (1 ng/kg i.c.v.) 2 h after ET-1 induced MCAO. Individual infarct volumes, together with mean ± SD, on the ipsilateral side measured 72 h post-stroke are shown for (D) cortical and (E) striatal regions for vehicle (n = 10), PcTx1 (n = 9), and inactive PcTx1 (n = 7). *P<0.05 versus vehicle (one-way ANOVA).

Figure 3. Behavioural performance after MCAO. The effect of vehicle (saline) (n = 10), PcTx1 (1 ng/kg i.c.v.; n = 9), and inactive PcTx1 (1 ng/kg i.c.v.; n = 7) on (A) percentage errors made in ledged beam test, and (B) neurological score following stroke. Ledged beam test and neurological assessment were performed pre-stroke (PS) and at 24 h (24) and 72 h (72) post-stroke. Data are mean ± SD. [##]P<0.01 versus pre-stroke performance; [**]P<0.01 versus corresponding time in vehicle-treated group (two-way RM ANOVA followed by Tukey post hoc tests).

Figure 4. Neuronal survival after MCAO. (A) Effect of vehicle (n = 10), PcTx1a (1 ng/kg i.c.v.; n = 9), and inactive PcTx1 (1 ng/kg i.c.v.; n = 7) on neuronal survival measured 72 h post-stroke. Data expressed as the number (mean ± SD) of NeuN-immunopositive (NeuN^{+}) cells per mm[2] within the non-occluded (contralateral) and occluded (ipsilateral) hemisphere. #P<0.05 versus

vehicle-treated group (ipsilateral side); **P<0.01 versus matched region on non-infarcted hemisphere (two-way ANOVA followed by Tukey post hoc tests); (B) Representative immunohistochemical brain sections depicting neuronal expression using NeuN neuronal marker (green). Images are taken from either the non-occluded or occluded hemisphere from animals that were stroked and subsequently treated with vehicle, PcTx1 or inactive PcTx1.

Figure 5. Apoptosis after MCAO. (A) Effect of vehicle (n = 10), PcTx1 (1 ng/kg i.c.v.; n = 9) or inactive PcTx1 (1 ng/kg i.c.v.; n = 7) on the number of cells undergoing apoptosis at 72 h post-stroke. Data expressed as the number (mean ± SD) of cleaved caspase-3-immunopositive (caspase-3^{+}) cells per mm^{2} area within the non-occluded (contralateral) and occluded (ipsilateral) hemisphere. **P<0.01 versus matched region on non-infarcted hemisphere (two-way ANOVA followed by Tukey post hoc tests); (B) Representative immunohistochemical brain sections depicting neuronal expression using a marker for cleaved caspase-3 (red). Images are taken from either the non-occluded or occluded hemisphere from animals that were stroked and subsequently treated with vehicle, PcTx1 or inactive PcTx1.
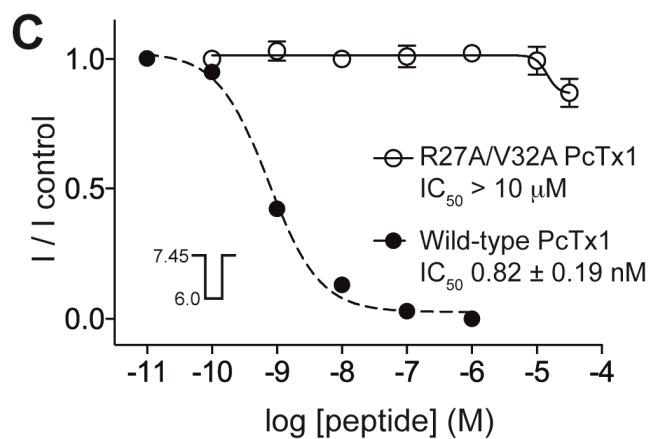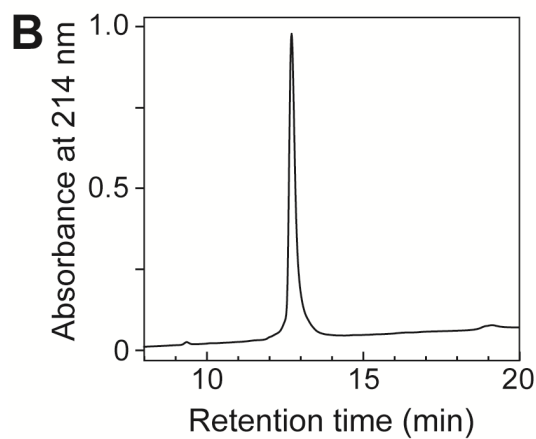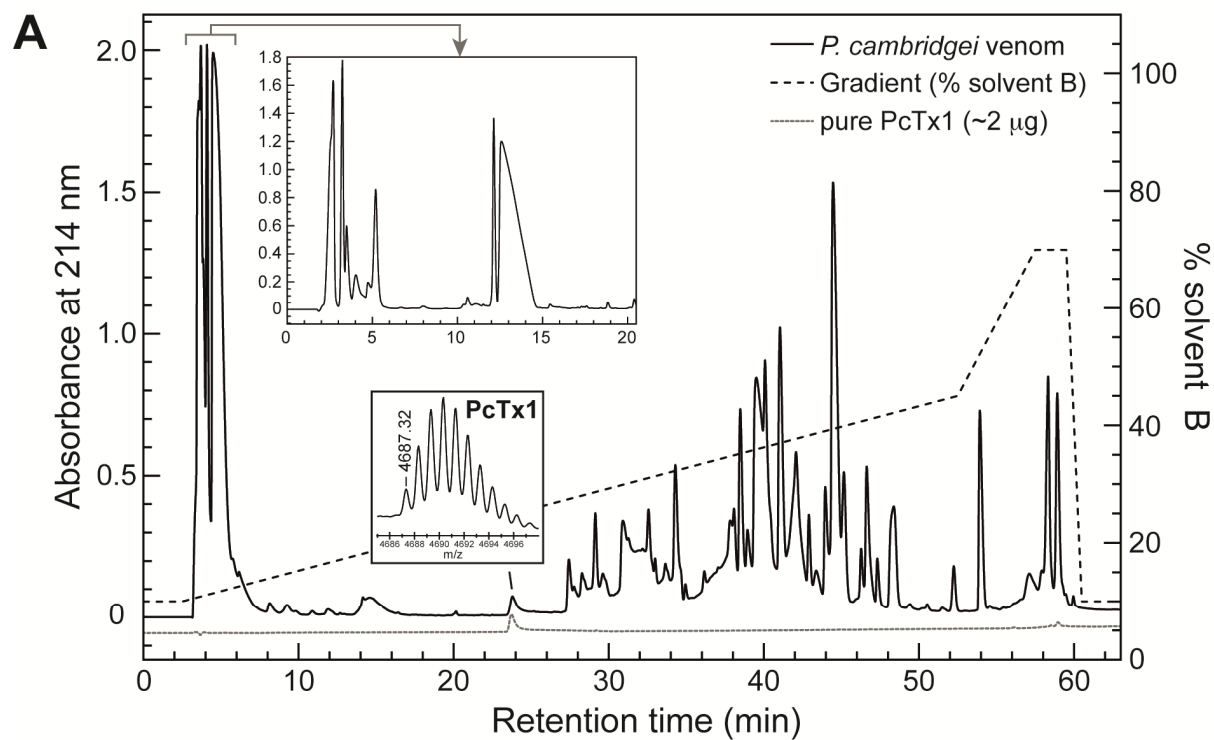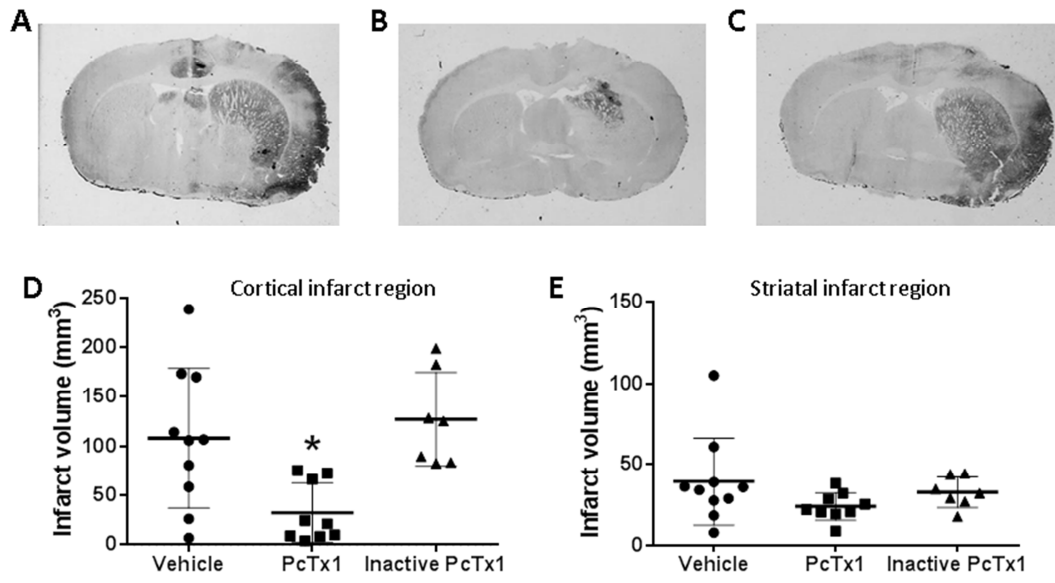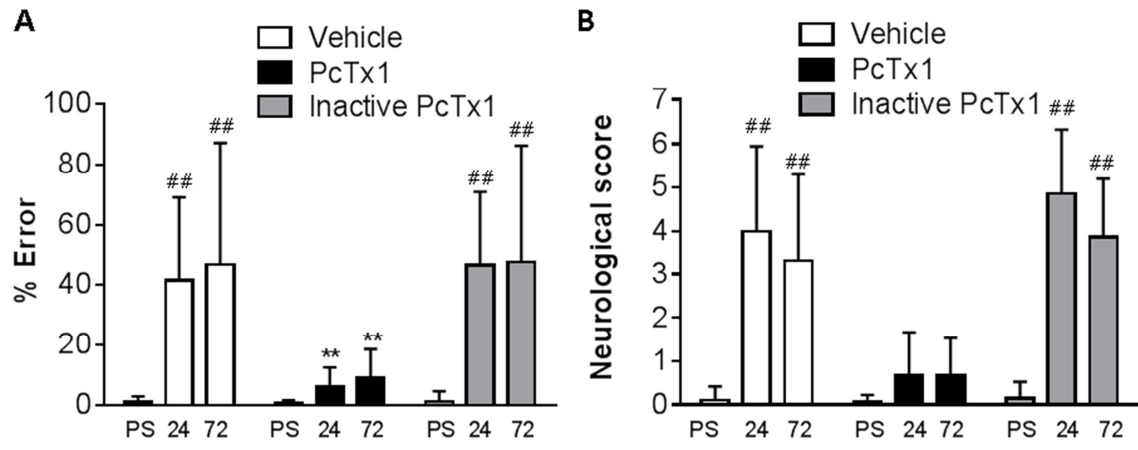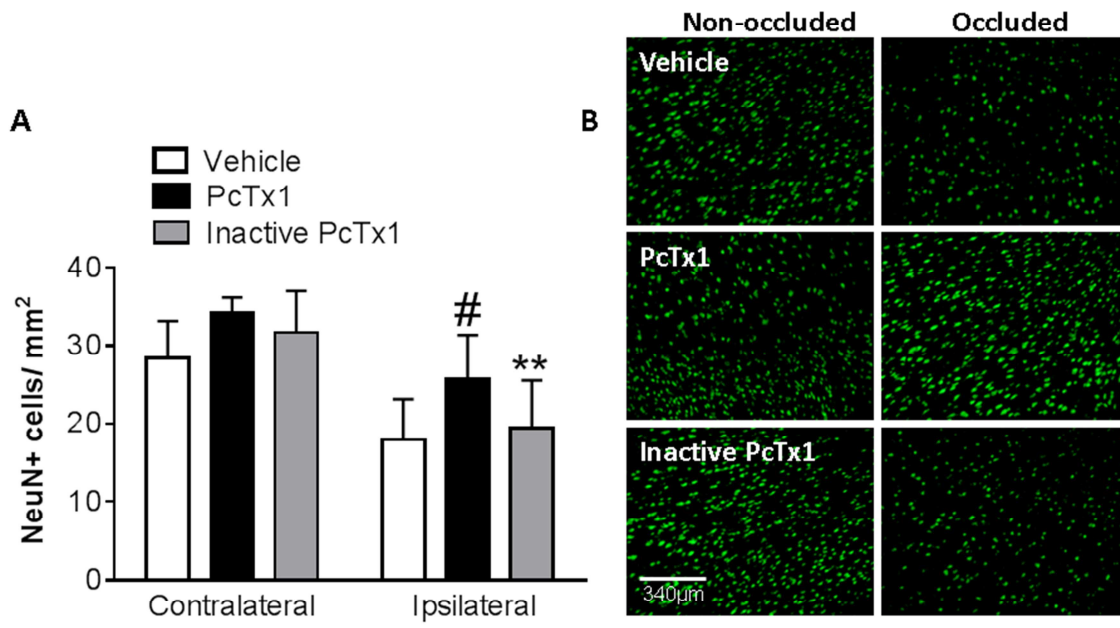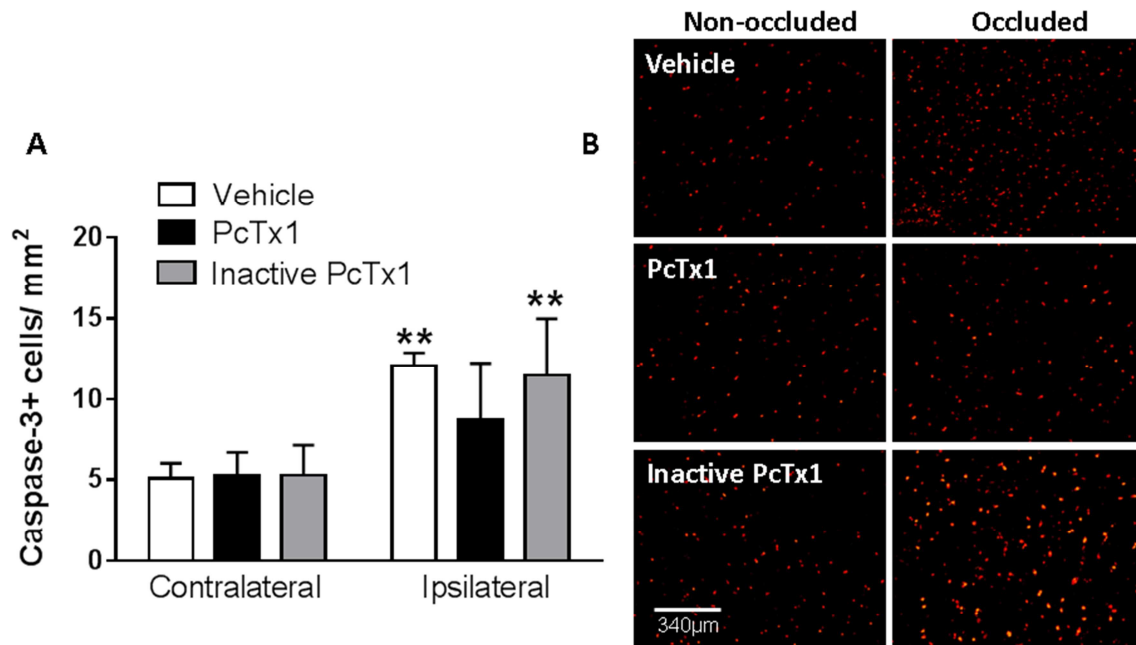
Highlights

- The effect of pure PcTx1 to inhibit ASIC1a was tested in a hypertensive model of stroke
- PcTx1 evoked neuroprotection when administered centrally after stroke
- PcTx1 reduced cortical infarcts and improved motor function tested after 3 days
- PcTx1 preserved neuronal architecture
- An inactive PcTx1 analog had no effect on stroke outcome